Available online at www.sciencedirect.com
SCIENCE DIRECT®
International Journal of Heat and Mass Transfer 48 (2005) 4835–4845
International Journal of HEAT and MASS TRANSFER
www.elsevier.com/locate/ijhmt

Dual mixed convection flows in a vertical channel

A. Barletta [a], E. Magyari [b,*], B. Keller [b]

[a] Dipartimento di Ingegneria Energetica, Nucleare e del Controllo Ambientale (DIENCA), Università di Bologna, Via dei Colli 16, I-40136 Bologna, Italy
[b] Chair of Physics of Buildings, Institute of Building Technology, Swiss Federal Institute of Technology (ETH) Zürich, CH-8093 Zürich, Switzerland

Received 29 April 2004; received in revised form 29 April 2005
Available online 15 August 2005

Abstract

The classical problem of the fully developed mixed convection flow with frictional heat generation in a vertical channel bounded by isothermal plane walls having the same temperature is revisited in this paper. The existence of dual solutions of the local balance equations is pointed out. They are either columnar upflows or cellular down–up–down flows. Below a maximum value $\Xi_{\max}$ of the governing parameter $\Xi = Ge\,Pr\,Re$ (the product of the Gebhart, Prandtl and Reynolds numbers), for any given Ξ a pair of different solutions occurs. The value $\Xi_{\max}$ corresponds to a maximum value of the Reynolds number above which no laminar solution can be found. At this maximum value, the two solution branches bifurcate from each other. In the neighborhood of the bifurcation point $\Xi_{\max}$ even small perturbations can cause transitions from one flow regime to the other. In the paper, the mechanical and thermal characteristics of the dual flow regimes are discussed in detail both analytically and numerically.

Keywords: Mixed convection; Vertical channel; Dual solutions; Bifurcation point; Viscous dissipation; Heat transfer

1. Introduction

Buoyancy induced flows in ducts deserve wide attention mainly for their engineering applications in several thermal control devices ranging from electronics to nuclear plants. Indeed, in passive or semi-passive thermal control systems, either purely free convection flows or mixed convection flows are involved.

Obtaining analytical solutions for mixed convection problems in vertical or inclined ducts has been the subject of several papers in the latter decades [1–5]. The importance of such analytical solutions, which refer to laminar fully developed flows, relies on the chance to obtain non-trivial benchmarks to test the reliability of numerical codes developed for more complex geometries or for non-parallel flows. Moreover, analytical solutions are often an opportunity to inspect the internal consistency of the mathematical models and of the approximations adopted, as well as to develop new theoretical results. For instance, in Ref. [5], a novel criterion to choose the reference temperature when adopting the Boussinesq approximation in duct flows has been proposed.

The theoretical investigations on fully developed mixed convection in vertical or inclined ducts are often devoted to a description of the changes on the velocity profiles induced by buoyancy as well as to the

* Corresponding author. Tel.: +41 01 6332867; fax: +41 01 6331041.
E-mail address: magyari@hbt.arch.ethz.ch (E. Magyari).

0017-9310/$ - see front matter © 2005 Elsevier Ltd. All rights reserved.
doi:10.1016/j.ijheatmasstransfer.2005.05.036

Nomenclature

A_n	dimensionless coefficients, Eq. (28)
B_n	dimensionless coefficients, Eq. (33)
Br	Brinkman number, $= \mu U_m^2/[k(T(0)-T_0)]$, Eq. (45)
c_p	specific heat at constant pressure
g	acceleration due to gravity
Ge	Gebhart number, $= 4Lg\beta/c_p$, Eq. (16)
h	dimensionless heat transfer coefficient, Eq. (44)
k	thermal conductivity
L	channel half-width
p	pressure
P	difference between the pressure and the hydrostatic pressure
Pr	Prandtl number, $= \mu c_p/k$, Eq. (16)
Re	Reynolds number, $= 4LU_m/\nu$, Eq. (16)
Re_{max}	maximum allowed value of Re
T	temperature
T_0	wall temperature
T_r	reference temperature
u	dimensionless velocity, $= U/U_m$, Eq. (16)
U	X-component of the fluid velocity
U_m	mean fluid velocity, Eq. (10)
$\mathbf{V}$	fluid velocity vector
X, Y	Cartesian coordinates
y	dimensionless transversal coordinate
Greek symbols	
α	dimensionless parameter, $= \mathrm{d}\phi/\mathrm{d}y\|_{y=0}$, Eq. (26b)
β	coefficient of thermal expansion
ϕ	dimensionless velocity gradient, $= (\Xi/16)\mathrm{d}u/\mathrm{d}y$, Eq. (21)
λ	dimensionless parameter, $= -(1/\Xi)\mathrm{d}\phi/\mathrm{d}y\|_{y=1}$, Eq. (42)
μ	dynamic viscosity
ν	kinematic viscosity, $\nu = \mu/\rho$
ρ	mass density evaluated at the reference temperature
Ξ	dimensionless parameter, $= Ge\,Pr\,Re$, Eq. (16)
Ξ_{max}	maximum allowed value of Ξ

determination of the conditions for the onset of flow reversal (crossover from a columnar to a cellular flow). Indeed, the flow reversal phenomenon arises when buoyancy forces are so strong that there exists a domain within the duct where the local fluid velocity has a direction opposite to the mean fluid flow. These studies are often based on the assumption that the effect of viscous dissipation in the fluid is negligible. This assumption holds whenever the fluid has a sufficiently high thermal conductivity, a sufficiently small Prandtl number and sufficiently high wall heat fluxes are present. On the other hand, other theoretical investigations have been devoted to the analysis of the interplay between the effect of viscous dissipation and the effect of buoyancy [6–14]. These theoretical studies present either analytical or numerical solutions of the local momentum balance equations under the Boussinesq approximation. From a mathematical point of view, viscous heating is represented by a non-linear term (the dissipation function) in the local energy balance equation. Non-linearities due both to inertia and to viscous heating are usually neglected when studying fully developed mixed convection flows in vertical channels. As a consequence, the analysis of such flows allows for a straightforward analytical determination of the velocity and temperature profiles. However, when viscous heating is present, the solutions to be determined are less simple and analytical methods based either on perturbation expansions or on non-linear extensions of the Frobenius method are needed. Perturbation solutions are obtained in Refs. [7,8,10–12] with reference to channel flows. The boundary conditions considered on the walls of the channel are either uniform temperature or uniform heat flux. As it is well known, the latter boundary conditions imply, in the fully developed region, a linearly varying wall temperature in the streamwise direction (when the viscous dissipation is neglected). Dealing with non-linear governing equations may imply non-uniqueness of the solution for a given set of boundary conditions. Examples of dual solutions have been discussed in Refs. [14,15] either for a clear fluid or for a fluid-saturated porous medium.

The aim of the present paper is to analyze combined forced and free flow in the fully developed region of a vertical channel with isothermal walls kept at the same temperature, the fluid properties being assumed as constant. The viscous dissipation effect will be taken into account. The set of governing balance equations will be reduced to a fourth-order ordinary differential equation for the velocity field which will be solved both analytically and numerically. The analytical method will be based on a power series expansion with respect to the transverse coordinate. It will be shown that dual solutions may arise for a prescribed mass flow rate. Comparisons with another approach to the same problem based on a perturbation method by the first author [10] will be performed.

2. Model and governing equations

We consider the laminar fully developed flow in a vertical channel bounded by isothermal plane walls both kept at a temperature T_0 (Fig. 1). The effect of viscous dissipation is taken into account and the Boussinesq approximation is adopted. A steady parallel flow regime is assumed, so that the velocity field is given by $\mathbf{V} = (U, 0, 0)$.

The local mass balance equation reduces in this case to $\partial U/\partial X = 0$ and implies $U = U(Y)$. The momentum balance according to the Boussinesq approximation yields

$$\mu \frac{\mathrm{d}^2 U}{\mathrm{d}Y^2} - \frac{\partial P}{\partial X} + \rho g \beta (T - T_\mathrm{r}) = 0, \quad \frac{\partial P}{\partial Y} = 0, \tag{1a, b}$$

where $P = p + g\rho X$ is the difference between the pressure p and the hydrostatic pressure $-g\rho X$. The density ρ, the dynamic viscosity μ and the thermal expansion coefficient β are evaluated at a (not yet specified) reference temperature T_r. The energy balance equation is

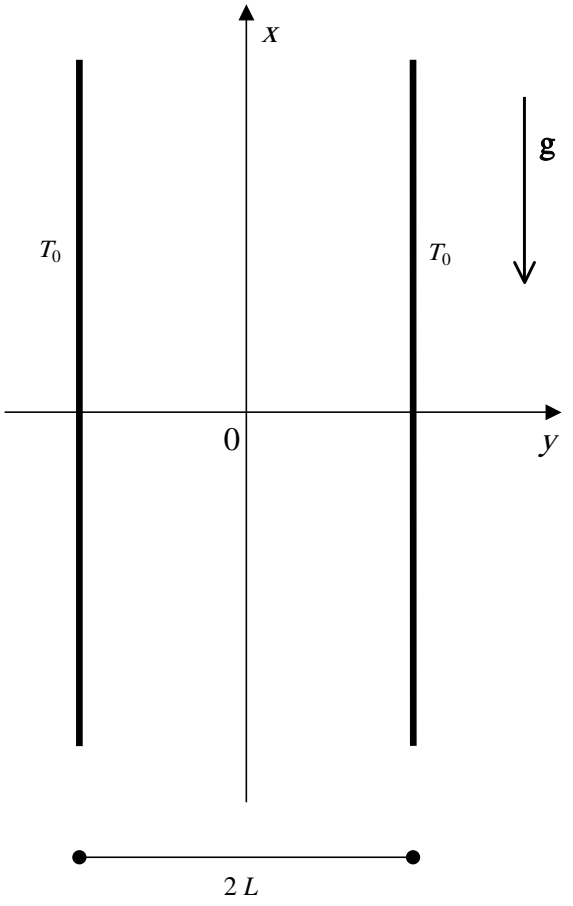

Fig. 1. Drawing of the channel.

$$k\left(\frac{\partial^2 T}{\partial X^2} + \frac{\partial^2 T}{\partial Y^2}\right) + \mu\left(\frac{\mathrm{d}U}{\mathrm{d}Y}\right)^2 = 0. \tag{2}$$

The no slip conditions and the thermal boundary conditions are

$$U|_{Y=\pm L} = 0, \quad T|_{Y=\pm L} = T_0. \tag{3a, b}$$

We restrict our considerations in the present paper to the solutions which are symmetric with respect to the midplane $Y = 0$ of the channel. The possible existence of non-symmetric flows in a channel bounded by isothermal walls kept at the same temperature is beyond the scope of the present paper. Accordingly, on the midplane $Y = 0$, the symmetry conditions

$$\left.\frac{\mathrm{d}U}{\mathrm{d}Y}\right|_{Y=0} = 0, \quad \left.\frac{\partial T}{\partial Y}\right|_{Y=0} = 0, \tag{4a, b}$$

will be imposed.

Eq. (1b) implies $P = P(X)$. Eq. (1a) solved with respect to T yields

$$T = T_\mathrm{r} + \frac{1}{\rho g \beta}\frac{\mathrm{d}P}{\mathrm{d}X} - \frac{\mu}{\rho g \beta}\frac{\mathrm{d}^2 U}{\mathrm{d}Y^2}. \tag{5}$$

The boundary conditions (3b) and Eq. (5) imply that $\mathrm{d}P/\mathrm{d}X =$ constant and thus, similarly to the velocity U, the temperature T depends only on the transverse coordinate, i.e., $T = T(Y)$. The above assumed symmetry implies that it is sufficient to seek the solution only in the half-channel $0 \leqslant Y \leqslant L$. Thus, the set of governing equations become

$$\mu \frac{\mathrm{d}^2 U}{\mathrm{d}Y^2} - \frac{\mathrm{d}P}{\mathrm{d}X} + \rho g \beta (T - T_\mathrm{r}) = 0, \tag{6}$$

$$k\frac{\mathrm{d}^2 T}{\mathrm{d}Y^2} + \mu\left(\frac{\mathrm{d}U}{\mathrm{d}Y}\right)^2 = 0, \tag{7}$$

$$U(L) = 0, \quad T(L) = T_0, \tag{8a, b}$$

$$\left.\frac{\mathrm{d}U}{\mathrm{d}Y}\right|_{Y=0} = 0, \quad \left.\frac{\mathrm{d}T}{\mathrm{d}Y}\right|_{Y=0} = 0. \tag{9a, b}$$

The general solution of Eqs. (6) and (7) for U and T involves four constants of integration in addition to the unknown value of the constant pressure gradient $\mathrm{d}P/\mathrm{d}X$. Hence the four boundary conditions (8) and (9) are not sufficient to determine these five unknown quantities. In other words, from a mathematical point of view Eqs. (6)–(9) represent an ill-posed (underdefined) boundary value problem. Therefore, an additional constraint must be given in order to determine the solution $\{U, T, \mathrm{d}P/\mathrm{d}X\}$ of Eqs. (6)–(9). It is common practice in duct flow studies to assume the mass flow rate as a prescribed quantity. Hence, in the following, the average fluid velocity in a channel section, namely

$$U_\mathrm{m} = \frac{1}{2L}\int_{-L}^{L} U(Y)\,\mathrm{d}Y = \frac{1}{L}\int_0^L U(Y)\,\mathrm{d}Y, \tag{10}$$

will be considered as being prescribed.

Eqs. (6) and (7) result in an ordinary differential equation of the fourth order for U

$$\frac{d^4U}{dY^4} = \frac{\rho g\beta}{k}\left(\frac{dU}{dY}\right)^2. \tag{11}$$

Eqs. (8a), (9a) and (9b), in the latter case by taking into account Eq. (5), lead to the following three boundary conditions for $U(Y)$

$$U(L) = 0, \tag{12}$$

$$\left.\frac{dU}{dY}\right|_{Y=0} = 0, \quad \left.\frac{d^3U}{dY^3}\right|_{Y=0} = 0. \tag{13a, b}$$

As explained above, the missing fifth condition will be replaced by the constraint (10) on the value of the average velocity U_m. In this way, the problem (10)–(13) for $U = U(Y)$ becomes well posed.

Once the velocity $U = U(Y)$ has been obtained, the temperature field can be determined by integrating Eq. (7) twice with respect to Y, namely

$$T(Y) = T_0 + \frac{\mu}{k}\int_Y^L \left\{\int_0^{\tilde{Y}} \left[\frac{dU(\overline{Y})}{d\overline{Y}}\right]^2 d\overline{Y}\right\} d\tilde{Y}. \tag{14}$$

Finally, after having obtained $U(Y)$ and $T(Y)$, one can find the value of the constant dP/dX from Eq. (6)

$$\frac{dP}{dX} = \mu\frac{d^2U(Y)}{dY^2} + \rho g\beta[T(Y) - T_r]. \tag{15}$$

The right-hand side of Eq. (15) must be independent of Y, so that it can be evaluated at any position in the range $0 \leqslant Y \leqslant L$.

The procedure described above, which allows one to obtain $U(Y)$, $T(Y)$ and dP/dX, leads to two important conclusions:

1. the fields $U(Y)$ and $T(Y)$ are determined without any need to fix the reference temperature T_r in the momentum balance equation;
2. the dimensional constant dP/dX depends on the choice of the reference temperature T_r.

3. Dimensionless parameters and solution procedure

Let us define the following dimensionless quantities:

$$u = \frac{U}{U_m}, \quad y = \frac{Y}{L}, \quad Ge = \frac{4Lg\beta}{c_p}, \quad Pr = \frac{\mu c_p}{k}, \quad Re = \frac{4LU_m}{\nu}, \quad \Xi = GePrRe, \tag{16}$$

where the Gebhart and Reynolds numbers are defined with respect to the hydraulic diameter $4L$ of the channel.

The limiting case $\Xi \to 0$ may correspond either to a very small viscous dissipation heating or to negligible buoyancy effects. In the problem under exam, these limiting cases are physically related since buoyancy forces are generated by the viscous dissipation effect in the fluid. Indeed, the latter effect is significant only if the average velocity U_m is not too small. By employing the dimensionless quantities defined in Eq. (16), the boundary value problem (10)–(13) can be rewritten as follows:

$$\frac{d^4u}{dy^4} = \frac{\Xi}{16}\left(\frac{du}{dy}\right)^2, \tag{17}$$

$$u|_{y=1} = 0, \quad \left.\frac{du}{dy}\right|_{y=0} = 0, \quad \left.\frac{d^3u}{dy^3}\right|_{y=0} = 0, \tag{18a, b, c}$$

$$\int_0^1 u(y)\,dy = 1. \tag{19}$$

It can be easily verified that, in the limiting case $\Xi \to 0$, Eqs. (17)–(19) admit a unique solution, namely

$$u(y) = \frac{3}{2}(1 - y^2). \tag{20}$$

Eq. (20) represents the well known Poiseuille velocity profile which is the expected limit when buoyancy forces become negligible.

When $\Xi \neq 0$, the solution of Eqs. (17)–(19) can be found both analytically and numerically. Since Eq. (17) involves only the derivatives of the dimensionless velocity $u(y)$ and thus it is convenient to introduce the dimensionless function $\phi = \phi(y)$,

$$\phi(y) = \frac{\Xi}{16}\frac{du(y)}{dy}. \tag{21}$$

In this way, Eqs. (17)–(19) lead to the boundary value problem

$$\frac{d^3\phi}{dy^3} = \phi^2, \tag{22}$$

$$\phi|_{y=0} = 0, \quad \left.\frac{d^2\phi}{dy^2}\right|_{y=0} = 0, \tag{23a, b}$$

$$\int_0^1 \left[\int_y^1 \phi(\bar{y})\,d\bar{y}\right] dy = -\frac{\Xi}{16}. \tag{24}$$

A procedure to determine the solution of Eqs. (22)–(24) can be based for instance on a shooting method. To this end, one first adds to Eqs. (23) formally the "missing" initial conditions for $d\phi/dy$ on $y = 0$. In this way, one gets the well posed initial value problem

$$\frac{d^3\phi}{dy^3} = \phi^2, \tag{25}$$

$$\phi(0) = 0, \quad \left.\frac{d\phi}{dy}\right|_{y=0} = \alpha, \quad \left.\frac{d^2\phi}{dy^2}\right|_{y=0} = 0. \tag{26a, b, c}$$

which, however, involves the arbitrary parameter α. Then, by letting α vary over the real axis, one obtains

a one-parameter family of solutions $\phi(y;\alpha)$ each of which corresponding to a specific value of Ξ that can be obtained by using Eq. (24). Through this method, a function $\Xi(\alpha)$ has been defined. In the next chapter, it will be shown that the function $\Xi = \Xi(\alpha)$ is non-monotonic, i.e., the same value of Ξ may correspond to a pair of different values of α. As a consequence, one can conclude that the solution of Eqs. (22)–(24) for a given Ξ may be not unique, but dual solutions may arise.

4. Analytical and numerical solution

4.1. Analytical solution

Let us look for the solution of Eqs. (25) and (26) in the form of a power series of y

$$\phi(y;\alpha) = \sum_{n=0}^{\infty} A_n(\alpha) y^n. \tag{27}$$

Thus, by substituting Eq. (27) into Eq. (25), we obtain the following recursion equations for the coefficients $A_n(\alpha)$:

$$A_{n+3}(\alpha) = \frac{n!}{(n+3)!} \sum_{k=0}^{n} A_k(\alpha) A_{n-k}(\alpha), \quad n = 0, 1, 2, 3, \ldots \tag{28}$$

Now, the "initial conditions" $\phi(0) = 0$, $\phi'(0) = \alpha$ and $\phi''(0) = 0$ imply $A_0(\alpha) = 0$, $A_1(\alpha) = \alpha$ and $A_2(\alpha) = 0$, respectively. Thus, from Eqs. (23) one easily infers that the only non-vanishing coefficients of the series (27) are $A_1(\alpha) = \alpha$, $A_5(\alpha)$, $A_9(\alpha)$, $A_{13}(\alpha)$, $A_{17}(\alpha), \ldots$, i.e., $A_{4n+1}(\alpha)$, for $n = 0, 1, 2, 3, \ldots$ Moreover, all the coefficients of higher order, $A_5(\alpha)$, $A_9(\alpha)$, $A_{13}(\alpha), \ldots$ can be calculated in terms of $A_1(\alpha) = \alpha$ successively. For the first of them, we obtain:

$$\begin{aligned}
A_5(\alpha) &= \frac{2!}{5!} A_1(\alpha)^2 = \frac{\alpha^2}{60}, \\
A_9(\alpha) &= \frac{6!}{9!} [A_1(\alpha) A_5(\alpha) + A_5(\alpha) A_1(\alpha)] = \frac{\alpha^3}{15120}, \\
A_{13}(\alpha) &= \frac{10!}{13!} [A_1(\alpha) A_9(\alpha) + A_5(\alpha)^2 + A_9(\alpha) A_1(\alpha)] \\
&= \frac{31\alpha^4}{129729600}, \\
A_{17}(\alpha) &= \frac{14!}{17!} [A_1(\alpha) A_{13}(\alpha) + A_5(\alpha) A_9(\alpha) \\
&\quad + A_9(\alpha) A_5(\alpha) + A_{13}(\alpha) A_1(\alpha)] \\
&= \frac{29\alpha^5}{44108064000}, \\
&\vdots
\end{aligned} \tag{29}$$

Thus, by putting $n \to 4n - 2$ in Eq. (28) we obtain for the non-vanishing coefficients with $n > 1$ the recursive relation

$$A_{4n+1}(\alpha) = \frac{(4n-2)!}{(4n+1)!} \sum_{k=0}^{4n-2} A_k(\alpha) A_{4n-k-2}(\alpha), \quad n = 1, 2, 3, \ldots \tag{30}$$

However, on the right-hand site of Eq. (30), the first term $A_0(\alpha)A_{4n-2}(\alpha)$ and the last term $A_{4n-2}(\alpha)A_0(\alpha)$ are zero. Thus, Eq. (30) becomes

$$A_{4n+1}(\alpha) = \frac{(4n-2)!}{(4n+1)!} \sum_{k=1}^{4n-3} A_k(\alpha) A_{4n-k-2}(\alpha), \quad n = 1, 2, 3, \ldots \tag{31}$$

Eq. (29) suggest that it is convenient to substitute the coefficients $A_n(\alpha)$ with some new coefficients B_n defined by

$$A_{4n+1}(\alpha) = \alpha^{n+1} B_{4n+1}. \tag{32}$$

Thus, we obtain

$$B_1 = 1$$

and

$$B_{4n+1} = \frac{(4n-2)!}{(4n+1)!} \sum_{k=1}^{4n-3} B_k B_{4n-k-2}, \quad n = 1, 2, 3, \ldots \tag{33}$$

In this way, we have

$$\begin{aligned}
B_5 &= \frac{1}{60} = 1.66666 \times 10^{-2}, \\
B_9 &= \frac{1}{15120} = 6.61375 \times 10^{-5}, \\
B_{13} &= \frac{31}{129729600} = 2.38958 \times 10^{-7}, \\
B_{17} &= \frac{29}{44108064000} = 6.57476 \times 10^{-10}, \\
&\vdots
\end{aligned} \tag{34}$$

and the solution (27) of the initial value ϕ-problem (25) and (26) becomes

$$\phi(y;\alpha) = \sum_{n=0}^{\infty} B_{4n+1} \alpha^{n+1} y^{4n+1}. \tag{35}$$

Among the one-parameter family of solutions $\phi(y;\alpha)$, the solution of the boundary value problem (22)–(24) is selected by prescribing the constraint (24). On account of Eq. (35), this constraint can be rewritten as

$$\sum_{n=0}^{\infty} \frac{B_{4n+1}}{4n+3} \alpha^{n+1} = -\frac{\Xi}{16}. \tag{36}$$

The parameter α defined by Eq. (26b) can also be related via Eq. (21) to the second derivative of $u(y)$ evaluated in $y = 0$ as follows:

$$\frac{\alpha}{\Xi} = \frac{1}{16} \left. \frac{\mathrm{d}^2 u}{\mathrm{d}y^2} \right|_{y=0}. \tag{37}$$

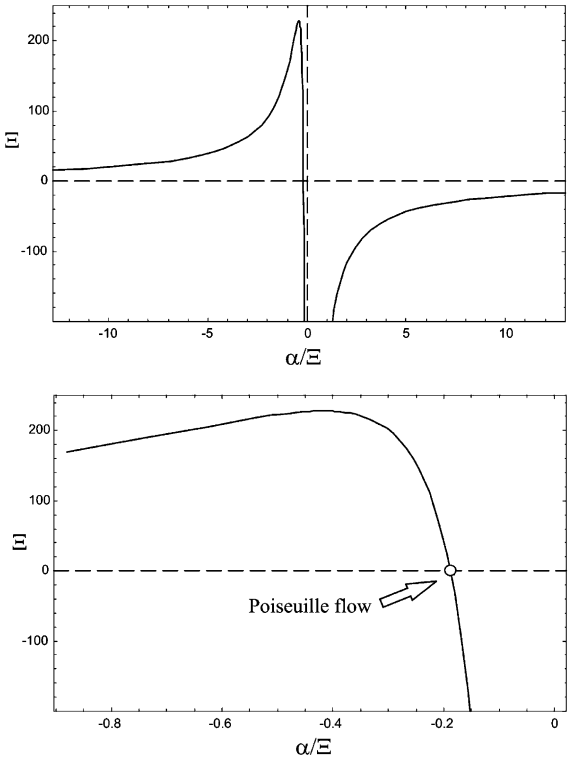

Fig. 2. Possible solutions of Eqs. (17)–(19) represented parametrically in the plane $(\alpha/\Xi, \Xi)$. The upper frame refers to the range $-12 < \alpha/\Xi < 12$, while the lower frame refers to $-1 < \alpha/\Xi < 0$.

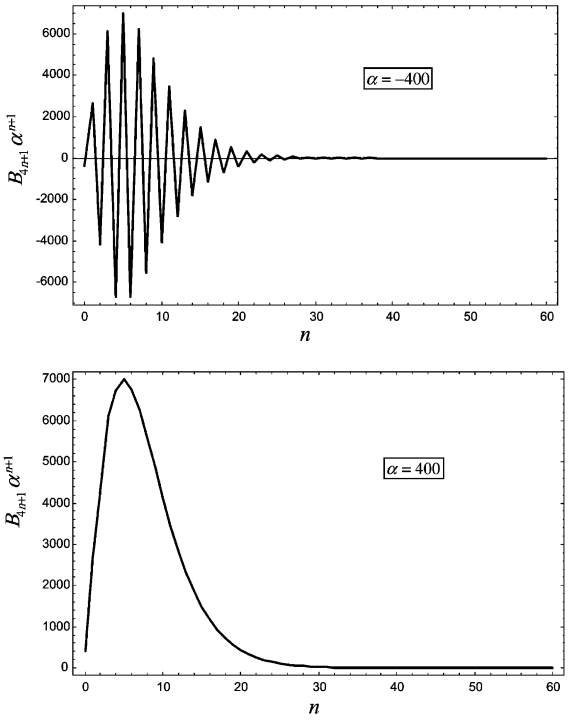

Fig. 3. First 60 coefficients $B_{4n+1}\alpha^{n+1}$ of the series given in Eq. (35) plotted for $\alpha = -400$ (upper frame) and for $\alpha = 400$ (lower frame).

Eqs. (20) and (37) imply that, in the limit $\Xi \to 0$, the ratio α/Ξ tends to $-3/16 = -0.1875$. The constraint given by Eq. (36) defines the set of possible solutions of the boundary value problem (17)–(19). In Fig. 2, this set of solutions is represented parametrically in the plane $(\alpha/\Xi, \Xi)$. An analysis of this figure leads to the following inferences.

- There exists an absolute maximum for the parameter Ξ above which no solution is allowed. This absolute maximum is $\Xi = \Xi_{\max} = 228.12869$ and corresponds to the value $\alpha/\Xi = -0.41708747$.
- For $\Xi \to 0$, a unique value of α/Ξ and hence of d^2u/dy^2 at $y = 0$ exists. Indeed, in this limit, the curve representing the relation between α/Ξ and Ξ displays a horizontal asymptote for $\alpha/\Xi \to \pm\infty$.
- For each $\Xi \neq 0$ smaller than $\Xi_{\max}$, two different values of α/Ξ and hence of d^2u/dy^2 at $y = 0$ exist. As a consequence, dual solutions exist for every choice of $\Xi < \Xi_{\max}$, except for the limit $\Xi \to 0$, where the solution is unique (Poiseuille flow).

The convergence of the series solution expressed by Eq. (35) is very fast. In fact, in most cases, the first 60 terms in the expansion are sufficient to obtain more than 10 digits accuracy. A drawing of the trend of the coefficients in the series expansion (35) is given in Fig. 3. This figure refers to a pair of very extreme cases ($\alpha = -400$ and $\alpha = 400$) and reveals that the coefficients $B_{4n+1}\alpha^{n+1}$ tend to zero quite rapidly.

4.2. Numerical solution

The initial value problem (25) and (26) can easily be solved numerically by using any standard software package for ordinary differential equations as, for instance, *Mathematica 4.2* (©Wolfram Research, Inc.). The software allows one to get numerical solutions of ordinary differential equations through the use of the function `NDSolve`. The numerical solution and the analytical solution can be compared by testing the correspondence between α and Ξ. This correspondence is defined by the integral constraint (24) or, in the analytical solution, by Eq. (36). A comparison performed in the range $-250 \leqslant \alpha \leqslant -5$, reveals a complete agreement within six digits between the values of Ξ evaluated numerically and those evaluated analytically. Values of parameter Ξ in the range $-250 \leqslant \alpha \leqslant -5$ are reported in Table 1.

Table 1
Relation between parameters α and Ξ

α	Ξ	α	Ξ
−250	−191.085	−110	223.636
−230	−94.4847	−90	227.571
−210	−9.88583	−70	214.352
−190	62.6292	−50	182.017
−170	122.803	−30	128.118
−150	170.185	−10	49.6175
−130	204.103	−5	25.7262

5. Velocity distribution, temperature distribution and axial pressure gradient

From Eqs. (18a), (21) and (35), the dimensionless velocity $u(y)$ can be evaluated as

$$u(y) = -\frac{16}{\Xi}\int_y^1 \phi(y;\alpha)\,\mathrm{d}y = -\frac{16}{\Xi}\sum_{n=0}^{\infty}\frac{B_{4n+1}\alpha^{n+1}}{4n+2}(1-y^{4n+2}). \tag{38}$$

As a consequence of Eqs. (14), (16), (21), (33) and (35), the temperature field can be evaluated as

$$T(Y) = T_0 + \frac{256\mu U_\mathrm{m}^2}{k}\theta(y), \tag{39}$$

where $\theta(y)$ is a dimensionless function defined as

$$\theta(y) = \frac{1}{\Xi^2}\int_y^1\left[\int_0^{\bar{y}}\phi(\bar{y};\alpha)^2\,\mathrm{d}\bar{y}\right]\mathrm{d}\tilde{y} = \frac{1}{4\Xi^2}\sum_{n=0}^{\infty}\left[\sum_{m=0}^{n}B_{4m+1}B_{4(n-m)+1}\right]\times\frac{\alpha^{n+2}}{(4n+3)(n+1)}[1-y^{4(n+1)}] = \frac{1}{\Xi^2}\sum_{n=1}^{\infty}(4n+1)B_{4n+1}\alpha^{n+1}[1-y^{4n}]. \tag{40}$$

Function $\theta(y)$ can be considered as a dimensionless temperature.

Once the reference temperature T_r has been chosen, the constant $\mathrm{d}P/\mathrm{d}X$ can be evaluated by employing Eq. (15). Following Ostrach [6], one can set the reference temperature equal to the temperature of the static equilibrium state of the system, which in the present case means the wall temperature, $T_\mathrm{r} = T_0$. Then, by employing Eq. (15) with $Y = L$, together with Eqs. (16) and (21), one obtains

$$\frac{\mathrm{d}P}{\mathrm{d}X} = \mu\left.\frac{\mathrm{d}^2U}{\mathrm{d}Y^2}\right|_{Y=L} = \frac{16\mu U_\mathrm{m}}{L^2\Xi}\left.\frac{\mathrm{d}\phi}{\mathrm{d}y}\right|_{y=1} = -\frac{16\mu U_\mathrm{m}}{L^2}\lambda, \tag{41}$$

where the parameter λ, given by

$$\lambda = -\frac{1}{\Xi}\left.\frac{\mathrm{d}\phi}{\mathrm{d}y}\right|_{y=1}, \tag{42}$$

represents the dimensionless axial pressure gradient. On account of Eq. (35), the parameter λ can be expressed as

$$\lambda = -\frac{1}{\Xi}\sum_{n=0}^{\infty}(4n+1)B_{4n+1}\alpha^{n+1}. \tag{43}$$

Taking into account Eqs. (39) and (40), a dimensionless heat transfer coefficient h is obtained as

$$h = -\left.\frac{\mathrm{d}\theta}{\mathrm{d}y}\right|_{y=1} = \frac{4}{\Xi^2}\sum_{n=1}^{\infty}(4n+1)nB_{4n+1}\alpha^{n+1}. \tag{44}$$

The effect of viscous dissipation is characterized by the Brinkman number Br which can be defined as

$$Br = \frac{\mu U_\mathrm{m}^2/k}{T(0)-T_0}. \tag{45}$$

Thus, from Eqs. (39) and (40) one immediately obtains

$$\frac{1}{Br} = 256\theta(0) = \frac{256}{\Xi^2}\sum_{n=1}^{\infty}(4n+1)B_{4n+1}\alpha^{n+1}. \tag{46}$$

As a consequence of Eqs. (20), (21) and (40)–(46), in the limit $\Xi \to 0$, the dimensionless temperature $\theta(y)$ together with the parameters λ, h and Br can be expressed as

$$\theta(y) = \frac{1}{256}\int_y^1\left[\int_0^{\bar{y}}\left(\frac{\mathrm{d}u(\bar{y})}{\mathrm{d}\bar{y}}\right)^2\mathrm{d}\bar{y}\right]\mathrm{d}\tilde{y} = \frac{3(1-y^4)}{1024}, \tag{47}$$

$$\lambda = -\frac{1}{16}\left.\frac{\mathrm{d}^2u}{\mathrm{d}y^2}\right|_{y=1} = \frac{3}{16} = 0.1875, \tag{48}$$

$$h = -\left.\frac{\mathrm{d}\theta}{\mathrm{d}y}\right|_{y=1} = \frac{3}{256} = 0.01171875, \tag{49}$$

$$Br = \frac{1}{256\theta(0)} = \frac{4}{3} \cong 1.333333. \tag{50}$$

Eq. (47) predicts a non-uniform temperature profile. In fact, it is well known that, for a duct with isothermal walls, different behaviours are expected if the viscous dissipation effect is neglected or if this effect is taken into account. In the first case, the temperature profile far from the inlet section tends to become axially invariant and uniform. In the second case, the temperature far from the inlet section tends to assume a non-uniform axially invariant profile. Indeed, far from the inlet section, the thermal energy generated through viscous heating diffuses transversally through the fluid and is transferred to the external environment. This behaviour is well known and widely treated in the literature; it has been observed both in the case of forced convection and in the case of mixed convection.

6. Discussion of the results

In Section 4, it has been pointed out that, for a fixed non-vanishing value of the governing parameter Ξ lower

than $\Xi_{max} = 228.12869$, two possible solutions of the governing equations exist. The case $\Xi = 0$ corresponds to the Poiseuille flow solution. Indeed, the latter solution holds in the limit of negligible buoyancy effects, i.e., in the limit of forced convection. The set of allowed solutions is clearly represented in Fig. 2. This figure shows that there exists a *first branch* in the set of solutions which corresponds to the interval $-0.417087 \leqslant \alpha/\Xi < 0$ and to all the allowed values of Ξ, namely $\Xi \leqslant \Xi_{max}$. This first branch includes the Poiseuille flow solution. There exists also a *second branch* in the set of solutions which corresponds either to the interval $\alpha/\Xi \leqslant -0.417087$ or to the interval $\alpha/\Xi > 0$ and to all the allowed non-vanishing values of Ξ, namely $\Xi \leqslant \Xi_{max}$. Except for the case $\Xi = 0$, to each solution in the first branch there corresponds a solution in the second branch having the same value of Ξ. These dual solutions are different for any $\Xi < \Xi_{max}$, while they are coincident for $\Xi = \Xi_{max}$.

In Fig. 4, plots of $u(y)$ and $\theta(y)$ are reported for the case $\Xi = \Xi_{max}$. This figure shows that a slight flow reversal occurs next to the boundary wall ($y = 1$). Indeed, there exists a region in the neighborhood of $y = 1$ where the dimensionless velocity is negative, i.e., where the fluid flows in the direction opposite to the mean flow.

In Figs. 5 and 6, the dual solutions corresponding to $\Xi = 20$ and $\Xi = -20$ are represented. These figures show that, while for the first branch solution the dimensionless velocity field is only slightly different from the Poiseuille

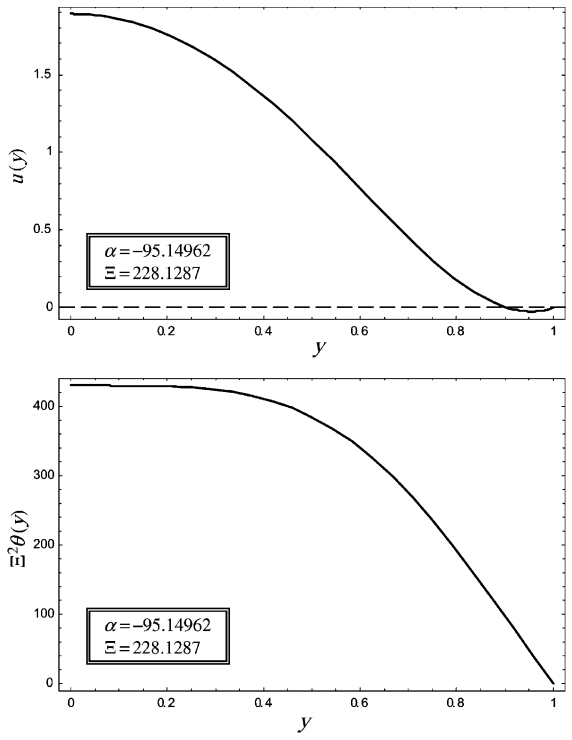

Fig. 4. Plots of $u(y)$ and $\Xi^2\theta(y)$, for $\Xi = \Xi_{max} = 228.1287$.

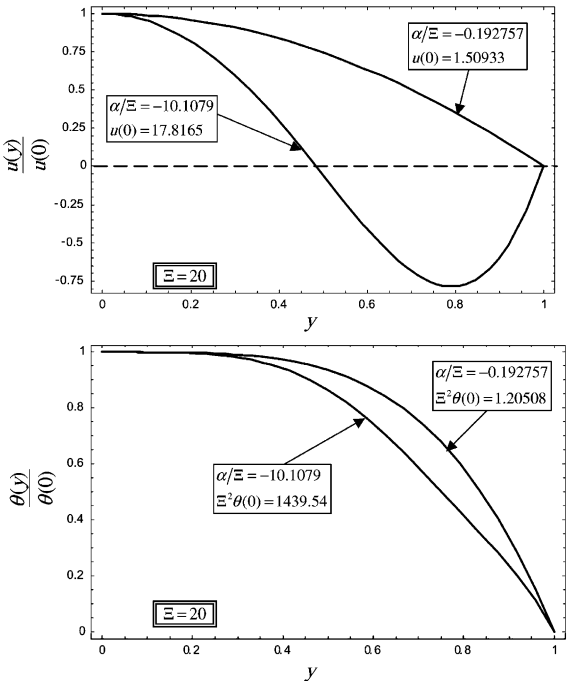

Fig. 5. Dual profiles of $u(y)/u(0)$ and $\theta(y)/\theta(0)$ for $\Xi = 20$.

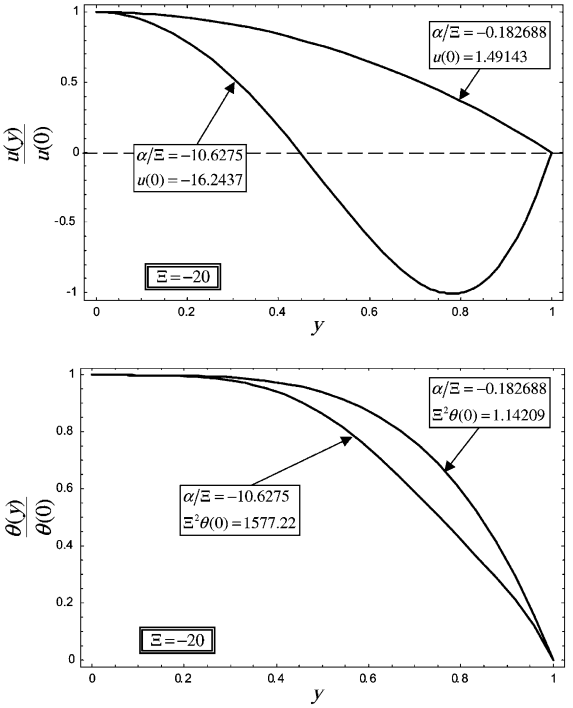

Fig. 6. Dual profiles of $u(y)/u(0)$ and $\theta(y)/\theta(0)$ for $\Xi = -20$.

Table 2
Values of Ge, Pr and Re_{max} for a channel with $L = 1$ cm

	Ge	Pr	Re_{max}
Water ($T_r = 293.15$ K)	1.970×10^{-8}	7.07	1.638×10^{9}
Unused engine oil ($T_r = 260$ K)	1.560×10^{-7}	1.45×10^{5}	1.012×10^{4}

velocity profile, the second branch solution yields a completely different velocity distribution. The latter displays a very strong flow reversal next to the boundary wall. The dimensionless temperature field for the first branch solution has a qualitative behavior similar to that for the second branch solution, but the values of θ are completely different. Indeed, the ratio between the values of $\theta(0)$ for the second branch solution and for the first branch solution is very high and increases rapidly as Ξ decreases.

The value Ξ_{max} is the upper bound of Ξ and is positive number, i.e., it corresponds to upward flow. This circumstance means that, in the case of upward flow, there exists a critical value of the Reynolds number which cannot be exceeded, namely

$$Re_{max} = \frac{\Xi_{max}}{Ge\,Pr} = \frac{228.12869}{Ge\,Pr}. \tag{51}$$

Eq. (51) implies that there exists a maximum average velocity $U_m^{(max)}$ for upward flow. On the other hand, no restrictions are implied by Fig. 2 for downward flow. Some data for a channel with $L = 1$ cm and for two different fluids are given in Table 2. These data show that, in most practical cases, the critical value Re_{max} is very high. In fact, the flow is expected to become turbulent for values of Re much lower than Re_{max}.

The differences between the first branch solution and the second branch solution corresponding to the same value of Ξ become smaller as the value of Ξ approaches its threshold value Ξ_{max}. As a consequence, when Ξ is in the neighborhood of Ξ_{max}, the differences between the dual solutions are so small that even a minor external perturbation may cause stochastic oscillations between one solution and the other. As pointed out above, this kind of instability is unlikely to be revealed since other instabilities exist for much smaller values of Ξ. Indeed, a doubling of the solution corresponding to a given value of Ξ occurs even if Ξ is not in the vicinity of the threshold value. However, when Ξ is much smaller than the threshold value, the differences occurring between the dual solutions are so significant that only major external disturbances may cause the transition from one flow regime to the other.

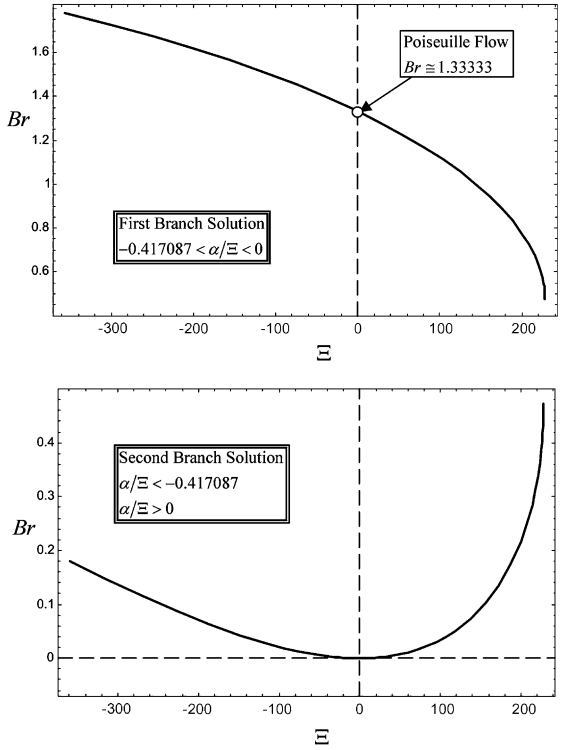

Fig. 7. Plots of Br versus Ξ for the first branch solution and for the second branch solution.

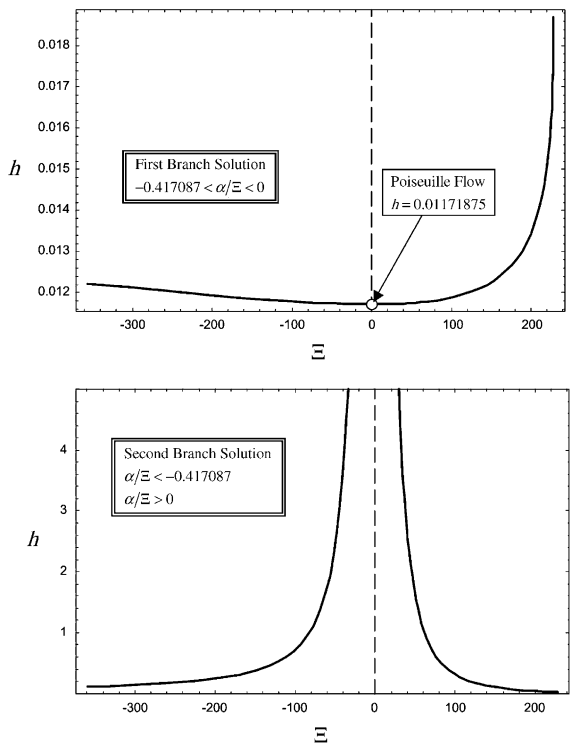

Fig. 8. Plots of h versus Ξ for the first branch solution and for the second branch solution.

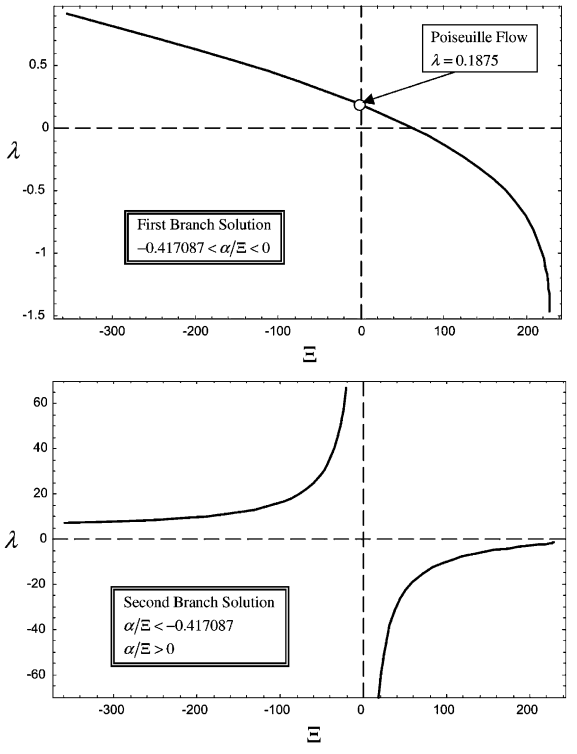

Fig. 9. Plots of λ versus Ξ for the first branch solution and for the second branch solution.

Figs. 7–9 display the behavior of the dimensionless quantities Br, h and λ versus Ξ with reference either to the first branch solution or to the second branch solution. Fig. 7 shows that the Brinkman number evaluated through the first branch solution is a decreasing function of Ξ, while the behavior of Br versus Ξ for the second branch solution is non-monotonic. In Ref. [10], the values of Br versus Ξ for the same system have been evaluated through a perturbation method employing the Poiseuille flow as the base solution and Ξ as the perturbation parameter. A comparison between the values of Br evaluated in the present paper for the first branch solution and those evaluated in Ref. [10] reveals perfect agreement. However, the perturbation method allows one to obtain only the first branch solutions and only within the radius of convergence of the perturbation expansion, which has been estimated in Ref. [10] as $|\Xi| < 227$. It is an interesting circumstance that the estimated upper bound of the convergence set for the perturbation method almost coincide with the maximum allowed value of Ξ evaluated in the present paper, namely $\Xi_{\max} = 228.12869$. However, all the first branch solutions with $\Xi < -\Xi_{\max}$ are not covered by the perturbation method discussed in Ref. [10]. As is well known, the convergence domain of a perturbation method does not necessarily include all the possible solutions of a boundary value problem. This feature of the perturbation method is closely related to the following characteristic of analytic functions. An analytic function may coincide with its Laurent expansion around a given point only for a proper subset of its domain of definition.

Figs. 8 and 9 show that, for the second branch solution, the parameters h and λ are singular in the limit $\Xi \to 0$. These singularities correspond to the absence of a second branch solution for $\Xi = 0$. Parameter λ may exhibit negative values. These negative values correspond to flow regimes such that the quantity P, i.e., the difference between the pressure and the hydrostatic pressure, increases in the direction of the mean flow.

7. Concluding remarks

Mixed convection flow in a vertical channel with isothermal walls at a given temperature T_0 has been analyzed by taking into account the effect of viscous heating. The local mass, momentum and energy balance equations have been written according to the Boussinesq approximation, without fixing explicitly the reference temperature. The solution procedure revealed that neither the velocity field nor the temperature field is influenced by the choice of the reference temperature. On the other hand, a choice of the reference temperature was needed in order to determine the axial pressure gradient. The governing equations have led to a fourth-order ordinary differential equation for the dimensionless velocity field; it has been solved both by an analytical method and by a numerical method. The dimensionless solution depends on a unique dimensionless parameter, Ξ. This parameter coincides with the product of the Gebhart number, the Prandtl number and the Reynolds number. An analysis of the solutions of the governing equations has shown the following important features.

- The solution exists only for values of the parameter Ξ smaller than $\Xi_{\max} = 228.12869$. This circumstance implies that the Reynolds number has an upper bound.
- Except for the cases $\Xi = \Xi_{\max}$ and $\Xi = 0$, a pair of different solutions exists for any fixed value of Ξ. The case $\Xi = 0$ corresponds to a negligible Gebhart number, i.e., to a negligible buoyancy effect (forced convection). In the case $\Xi = 0$, the unique solution corresponds to the Poiseuille velocity profile.
- Two branches occur in the solution space. The first branch includes the Poiseuille flow solution. To each solution in the second branch there corresponds a solution in the first branch having the same value of Ξ. A comparison with a previous solution obtained with a perturbation method [10] reveals perfect agreement with the first branch solution. On the other hand, the second branch solutions could not be

found by employing perturbation methods. A significant element is the coincidence of the radius of convergence estimated for the perturbation method and the upper bound $\Xi_{\max} = 228.12869$ for the existence of solutions.

References

[1] W. Aung, G. Worku, Theory of fully developed combined convection including flow reversal, ASME J. Heat Transfer 108 (1986) 485–488.

[2] C.-H. Cheng, H.-S. Kou, W.-H. Huang, Flow reversal and heat transfer of fully developed mixed convection in vertical channels, J. Thermophys. Heat Transfer 4 (1990) 375–383.

[3] T.T. Hamadah, R.A. Wirtz, Analysis of laminar fully developed mixed convection in a vertical channel with opposing buoyancy, J. Heat Transfer 113 (1991) 507–510.

[4] A.S. Lavine, Analysis of fully developed opposing mixed convection between inclined parallel plates, Wärme Stoffübertragung 23 (1988) 249–257.

[5] A. Barletta, E. Zanchini, On the choice of the reference temperature for fully developed mixed convection in a vertical channel, Int. J. Heat Mass Transfer 42 (1999) 3169–3181.

[6] S. Ostrach, Laminar flows with body forces, in: F.K. Moore (Ed.), Theory of Laminar Flows, Princeton University Press, Princeton, 1964, pp. 528–718.

[7] P.M. Beckett, Combined natural- and forced-convection between parallel vertical walls, SIAM J. Appl. Math. 39 (1980) 372–384.

[8] P.M. Beckett, I.E. Friend, Combined natural and forced convection between parallel walls: developing flow at higher Rayleigh numbers, Int. J. Heat Mass Transfer 27 (1984) 611–621.

[9] S. Antony Raj, Thermodynamic analysis of viscous dissipation effects in natural convection flow, Acta Phys. Hung. 66 (1989) 117–126.

[10] A. Barletta, Laminar convection in a vertical channel with viscous dissipation and buoyancy effects, Int. Commun. Heat Mass Transfer 26 (1999) 153–164.

[11] A. Barletta, Heat transfer by fully developed flow and viscous heating in a vertical channel with prescribed wall heat fluxes, Int. J. Heat Mass Transfer 42 (1999) 3873–3885.

[12] D.B. Ingham, I. Pop, P. Cheng, Combined free and forced convection in a porous medium between two vertical walls with viscous dissipation, Transport Porous Media 5 (1990) 381–398.

[13] A.K. Al-Hadhrami, L. Elliott, D.B. Ingham, Combined free and forced convection in vertical channels of porous media, Transport Porous Media 49 (2002) 265–289.

[14] G. Wilks, J.S. Barmley, Dual solutions in mixed convection, Proc. Roy. Soc. Edinburgh 87A (1981) 349–358.

[15] J.H. Merkin, On dual solutions occurring in mixed convection in a porous medium, J. Eng. Math. 20 (1985) 171–179.